



ORIGINAL ARTICLE

Production of high-quality pyrolysis product by microwave-assisted catalytic pyrolysis of wood waste and application of biochar



Hui Guo ^a, Xiaojing Qin ^b, Song Cheng ^{c,d,*}, Baolin Xing ^{c,d,*}, Dengke Jiang ^e,
Weibo Meng ^c, Hongying Xia ^f

^a School of Materials Science and Engineering, Henan Polytechnic University, Jiaozuo 454003, China

^b School of Surveying and Land Information Engineering, Henan Polytechnic University, Jiaozuo 454003, China

^c College of Chemistry and Chemical Engineering, Henan Polytechnic University, Jiaozuo 454003, China

^d Collaborative Innovation Center of Coal Work Safety and Clean High Efficiency Utilization, Jiaozuo 454003, China

^e Chifeng Shanjin Silver and Lead CO., LTD, Chifeng, Inner Mongolia 025450, China

^f Faculty of Metallurgical and Energy Engineering, Kunming University of Science and Technology, Kunming 650093, China

Received 24 January 2023; accepted 26 April 2023

Available online 8 May 2023

KEYWORDS

Wood waste;
Microwave pyrolysis;
Biochar;
Adsorbent;
Methyl orange

Abstract Wood waste is employed as the feedstock for production of high-quality pyrolysis products such as bio-oil, bio-gas and biochar by microwave pyrolysis using $ZnCl_2$ and $Fe(NO_3)_3$ as additive at 400–800 °C. Pyrolysis temperature influences the yield of the pyrolysis products, which indicates that the yield of bio-gas increases and the yield of biochar decreases as pyrolysis temperature increases. The yield of the bio-oil is little influenced by pyrolysis temperature, which is restrained in the existence of $ZnCl_2$ and $Fe(NO_3)_3$. $ZnCl_2$ increases the furfural content in bio-oil. While $Fe(NO_3)_3$ promotes H_2 production during pyrolysis process. The maximum heating value of bio-gas produced at 800 °C is 12.26 MJ/Nm³. The added $ZnCl_2$ and $Fe(NO_3)_3$ increase the yield of the biochar, which also promote the formation of pore structure of biochar. The $ZnCl_2$ and $Fe(NO_3)_3$ are converted into ZnO and Fe_3O_4 onto biochar after pyrolysis, which could be used as the adsorbent and photocatalyst for methyl orange removal.

© 2023 The Author(s). Published by Elsevier B.V. on behalf of King Saud University. This is an open access article under the CC BY-NC-ND license (<http://creativecommons.org/licenses/by-nc-nd/4.0/>).

1. Introduction

Large-scale utilization of fossil fuel has already caused environmental problems and deteriorated air quality due to production a variety of toxic substances such as $NxOx$, SO_3 and $PM_{2.5}$ (Ge et al., 2020;

Yang et al., 2021). Besides, the toxic substances have posed severe risks to the human health (Zhang et al., 2021). Biomass belongs to the renewable energy, which can be converted into the fuels and valuable chemicals (Cherubini and Ulgiati, 2010). Therefore, biomass can generally replace the fossil fuel to reduce the environment pollution and ensure stable energy supply by the densification, anaerobic digestion,

* Corresponding authors.

E-mail addresses: cskmust@163.com (S. Cheng), baolinxing@hpu.edu.cn (B. Xing).

gasification, and baling combustion (Ouyang et al., 2019). Moreover, biomass has the advantages of the abundant resources, carbon neutrality and low cost of use (Li et al., 2019). Conversion biomass into energy and valuable product has attracted the attentions of many scholars (Robinson et al., 2015). Pyrolysis can convert biomass into three kinds of pyrolysis products such as bio-oil, biochar and bio-gas to recover chemical substance and calorific values of biomass feedstock at elevated temperatures under non-oxidizing conditions among many alternatives (Cheng et al., 2022). Besides, pyrolysis is more favorable for large-scale applications (Foong et al., 2020).

Microwave heat is the promising heating method due to the advantages of selective heating, non-contact material heating and energy saving (Tang et al., 2020; Cao et al., 2020). Microwave heat can promote the generation of high-quality liquid and gas fuel (Chen et al., 2016). Microwave heat can prevent the secondary reactions such as retrogressive and condensation reactions in the biomass pyrolysis process (Cheng et al., 2022). Besides, biomass with high moisture can contribute to improving its microwave adsorption capacity, which realizes the rapid heating of biomass during pyrolysis process (Cheng et al., 2017; Cheng et al., 2021). Microwave heat has promising application potential in both pilot scale and industrial scale for processing various of biomass (Abdelsayed et al., 2018). The empty oil palm can produce bio-oil with 74% of phenolic compounds by pyrolysis using microwave heat (Prashanth et al., 2020). Gautam et al. pointed out that bio-oil produced from macroalgae has little oxygen containing compound when microwave heat processes the macroalgae (Gautam et al., 2019). Based on the above analysis, microwave heat is the promising heating method for biomass pyrolysis.

Bio-oil obtained from microwave pyrolysis has high quality (Shi et al., 2013). However, it still has poor physicochemical properties such as large content of the oxygen, moisture and acid, and low content of valuable components (Reddy et al., 2019). These poor physicochemical properties of bio-oil make it difficult to produce fuels or chemicals as an intermediate product (Durak and Genel, 2020). Many researchers have tried different methods to improve the physicochemical properties of bio-oil (Cheng et al., 2022). Rolin et al. studied the influence of several inorganic salt additives on the catalytic pyrolysis of biomass (Rolin et al., 1983). The results show that adding additives can improve the quality of bio-oil. Besides, it can selectively enhance the specific reactions such as hydrocarbons and anhydrosugars to produce the desirable components. Since then, catalytic pyrolysis biomass technology has received extensive attention and various of additives for biomass catalytic pyrolysis have been developed. Pang et al. used $ZnCl_2$ as the additive to investigate its influence on microwave pyrolysis of pine powder. The analysis result indicates that $ZnCl_2$ can significantly reduce the pyrolysis temperature and simplify the resultant bio-oil composition (Pang et al., 2023). Lu et al. (2011) reported that the content of furfural and levoglucosenone in the bio-oil increases when $ZnCl_2$ is used as the additive in the biomass pyrolysis process (Lu et al., 2011). Stefanidis et al. reported that $ZnCl_2$ can increase the furfural content of bio-oil in microwave pyrolysis cellulose process (Stefanidis et al., 2011). Wang et al. (2019) used the $Fe(NO_3)_3$ as additive in the microwave-assisted pyrolysis, which indicates that $Fe(NO_3)_3$ can decrease the acidity, viscosity and water content in bio-oil (Nma et al., 2022). Song et al. (Song et al., 2000) pointed out that some major components in the bio-oil are concentrated in upper/bottom phases low density and water content using $Fe(NO_3)_3$ as the additive, respectively (Song et al., 2000). Xia et al. (2023) reported that the addition of $Fe(NO_3)_3$ improves the physicochemical properties of the bio-oil (Xia et al., 2023). Therefore, adding additives of the $Fe(NO_3)_3$ and $ZnCl_2$ can improve the quality of bio-oil in biomass catalytic pyrolysis process.

Wood is used for shelter forests against wind and fixing sand, commercial plantation, landscape engineering, and agricultural protection forest. A large amount of wood wastes (WS) are produced from the wood process, such as sawdust, wood cuttings, and sapwood. It needs to find an efficient method to utilize the WS, which can also provide the utilization method for other similar wastes. In this work, WS is employed as the raw material for production of valuable products by

microwave heat-assisted catalytic pyrolysis using $Fe(NO_3)_3$ and $ZnCl_2$ as the additive under different pyrolysis temperature. $Fe(NO_3)_3$ and $ZnCl_2$ are added in pyrolysis process, which also improve the dielectric properties of WS in the microwave field. The influence of the $Fe(NO_3)_3$ and $ZnCl_2$ on the physicochemical properties of the pyrolysis products is analyzed and investigated. Besides, the physicochemical properties of the pyrolysis products produced from different pyrolysis temperature are investigated and analyzed. $Fe(NO_3)_3$ and $ZnCl_2$ can be converted into the Fe_3O_4 and ZnO onto biochar to form valuable biochar-based magnetic adsorbent-photocatalyst after pyrolysis, which can be used in dye wastewater removal.

2. Experimental section

2.1. Materials

WS is obtained from the Jiangsu province, China, which is grinded and dried for pyrolysis. Ferric nitrate and zinc chloride are purchased from Tianjin Kemiou Chemical Reagent Co., LTD and Tianjin Zhiyuan Chemical Reagent Co. LTD, respectively. Methyl orange (MO) is purchased from Tianjin kemio Chemical Reagent Co., Ltd.

2.2. Methods

In a typical experiment, WS is mixed with $Fe(NO_3)_3$ and $ZnCl_2$ in the aqueous solution, which is stirred for 24 h. 20 g dried simple (WS/Fe/Zn) is put in the multimode microwave oven with pyrolysis temperature of 400–800 °C. The pyrolysis gas is collected from microwave oven, which is condensed by condenser pipe. The liquid is bio-oil in condenser pipe after condensation. Pyrolysis gas that is non-condensable is bio-gas, which is collected using the gas collection bag. The residue is biochar in microwave oven after pyrolysis. The yields of the bio-oil and biochar are measured based on their actual weight. The yield of the bio-gas is calculated according to mass balance.

2.3. Characterization

The bio-gas is analyzed by gas chromatography (GC-Trace1310). The bio-gas is analyzed using a TG-BOND Q packed column using a thermal conductivity detector (TCD) and the nitrogen as the carrier gas. The chemical composition of bio-oil is analyzed by gas chromatography/mass spectrometry (GC-MS, ISQ) with a TG-5MS polar capillary column (30 m × 0.25 mm × 0.25 μm). The oven sets a temperature programming, and the initial temperature of the oven is 50 °C and then rises up to 200 °C with the rate of 3 °C/min. Finally, it rises up to 200–280 °C. Scanning electronmicroscopy is used to analyze the surface microstructure of biochar. X-ray diffraction (XRD) analysis is performed using an X-ray diffractometer with a Cu Ka X-ray source under a voltage of 40 kV and a current of 40 mA, Japan (D/max-3B, Japan) (Hou et al., 2022). The pore structure parameters of the biochars are measured by an automatic adsorption apparatus (Autosorb-1-C, USA) using N_2 as the adsorbate at 77 K (Zeng et al., 2022).

2.4. Adsorption experiments

The adsorption experiments are conducted in erlenmeyer flasks. 100 mL MO solution is mixed with 0.1 g biochar with

different concentrations in volumetric flask, which is heated at 30 °C until adsorption equilibrium. The residual amount of MO is tested using the UV–Vis spectrophotometer. The adsorption amount (q_e) of MO on biochar in the adsorption isotherm is calculated as follows:

$$q_e = \frac{V(C_o - C_e)}{M} \quad (1)$$

where C_o is the initial MO concentration and C_e is the equilibrium MO concentration. M is the quality of biochar. V is volume of solution. The adsorption isotherm models of adsorption process are presented in Table S1.

2.5. Photocatalytic experiment

The biochar is mixed with MO solution in dark condition to eliminate its adsorption effect. The concentrations of the MO are 80–120 mg/L, respectively. The liquid–solid ratio of MO is 8, respectively. After, the suspension is put in the photocatalytic reactor and irradiated by UV light. The mixed solution is placed in a photocatalytic reactor with a magnetic stirring speed of 300 r/min. A 250 W Hg lamp with a wavelength range of 200–400 nm is used as the UV light source. Small amounts of mixed solution are removed from photocatalytic reactor at regular intervals. The photocatalytic reaction time is 120 min. The photocatalytic degradation efficiency of MO is calculated based on the following equation.

$$\eta = \frac{C_o - C_t}{C_o} 100\% \quad (2)$$

The η is MO degradation percentage of biochar.

3. Results and discussions

3.1. Heating curves of WS/Fe/Zn

The heating curves of the WS/Fe/Zn are shown in Fig. 1. As Fig. 1 shown, WS/Fe/Zn takes 9 min to reach 800 °C when the microwave power is 1000 W. When the microwave power increases to 2000 W, the heating time is reduced to 5 min to reach 800 °C. This result indicates that high microwave power

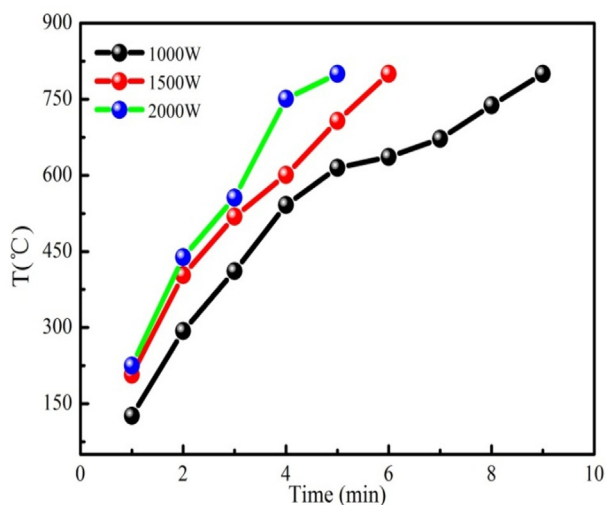


Fig. 1 The heating curves of WS/Fe/Zn.

can significantly reduce the heating time. The microwave power of 1500 W is used as the example to analyze the heating process of WS/Fe/Zn. Fig. 1 shows that the heating rate of WS/Fe/Zn is relatively slow at low temperature. The reason is that the organic volatile in WS/Fe/Zn has relatively low dielectric property. Besides, the absorbed microwave energy is primarily used to remove the moisture and preheat WS/Fe/Zn. Hemicellulose and cellulose begin to slowly decompose into bio-oil, bio-gas and preliminary biochar skeleton as heating time increases. The hemicellulose and cellulose in WS/Fe/Zn are rapidly decomposed or depolymerised producing low molecular weight volatiles at high pyrolysis temperature. The lignin of WS/Fe/Zn begins to decompose after 400 °C due to the formation of biochar. Biochar has good dielectric properties, which can rapidly adsorb the microwave energy for pyrolysis. Besides, ferric nitrate and zinc chloride are composed into the corresponding oxides, which contribute to WS/Fe/Zn pyrolysis in the microwave field. Therefore, the heating rate rapidly increases in the late heating period. WS/Fe/Zn has large heating rate at 1500 W. Therefore, 1500 W is selected for subsequent microwave pyrolysis experiment.

3.2. Distribution of pyrolysis products in existence of additive

Pyrolysis temperature plays an important role in the biomass pyrolysis process (Xie et al., 2014; Wang et al., 2016). Fig. 2 shows the distribution of pyrolysis products. As Fig. 2 shown, the yield of bio-oil increases at 400–600 °C. The bio-oil has the maximum yield of the 10.48% at 600 °C. However, the yield of the bio-oil decreases after 600 °C. It can be explained that high temperature favors to form bio-gas rather than bio-oil by secondary reactions, and the carbonization of volatiles for biochar would also decrease the yield of the bio-oil (Hou et al., 2022). The yield of the biochar decreases as pyrolysis temperature increases. It can be explained that the lignin in the WS/Fe/Zn is rarely decomposed at low pyrolysis temperature (Li et al., 2022). The yield of the bio-gas increases at 400–

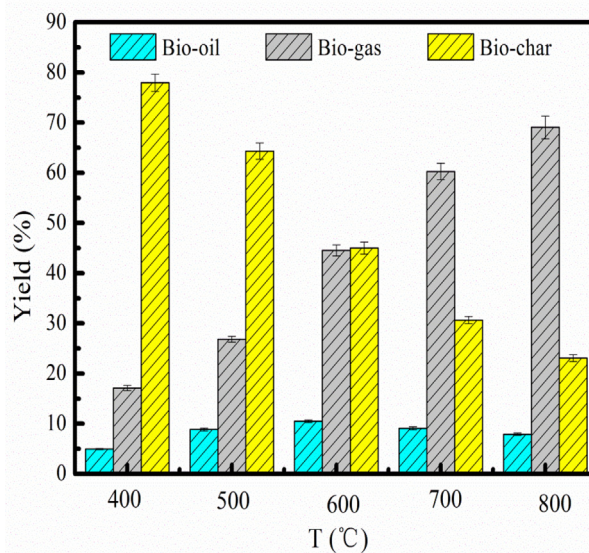


Fig. 2 Yield of pyrolysis product at different pyrolysis temperature.

800 °C. Bio-gas has the maximum yield at 800 °C, which is 69.05%. This result implies that microwave-assisted pyrolysis is the appropriate method to produce the bio-gas from organic waste (Ren et al., 2022). The reason is that high pyrolysis temperature contributes to converting volatile component into bio-gas (Kan et al., 2020). Besides, bio-char will be converted into bio-gas at high pyrolysis temperature. Xia et al. (2023) pointed out that $\text{Fe}(\text{NO}_3)_3$ promotes the polymerization and carbonization of the solid phase, accompanied by the release of small molecule gases as pyrolysis temperature increases, resulted in high yield of the bio-gas (Xia et al., 2023). WS/Fe/Zn pyrolysis without adding $\text{Fe}(\text{NO}_3)_3$ and ZnCl_2 at 400–800 °C is shown in Fig. S1. The yield of the bio-oil decreases and yield of the biochar increases compared to the WS/Fe/Zn pyrolysis without adding $\text{Fe}(\text{NO}_3)_3$ and ZnCl_2 . $\text{Fe}(\text{NO}_3)_3$ and ZnCl_2 can contribute to the some crosslinking or aromatization reactions in adjacent molecules, which are conducive to the production of biochar (Ryu et al., 2020). Besides, $\text{Fe}(\text{NO}_3)_3$ can promote the glycosidic bond breaking and water removal during pyrolysis process, which accelerates the formation of solid char. ZnCl_2 can improve the condensation reaction between aromatic hydrocarbons and bio-oil, and then promote the formation of macromolecules (polycyclic aromatic hydrocarbons) in the biochar during condensation reaction (Sun et al., 2018). These chemical reactions contribute to the generation of biochar, and restrain bio-oil generation (Ahmadpour and Do, 1997). Branca et al. reported that ZnCl_2 would catalyze the charring reactions, which contributes to producing more biochar and less volatile product during pyrolysis process (Branca et al., 2010). Oh et al. pointed out that the generation of bio-oil is inhibited when ZnCl_2 is added in the pyrolysis process (Oh et al., 2013). The desire pyrolysis temperature is chosen as 600 °C because of large bio-oil yield.

3.3. Bio-oil analysis

GC–MS is used to detect the composition of the bio-oil. Table 1 lists the composition of the bio-oil at different pyrolysis temperature. The bio-oil produced at 400 °C has large content of furfural, which is 17.08% (Table 1). However, the content of furfural is decrease as pyrolysis temperature increases, indicating that pyrolysis temperature significantly influences the content of furfural. It can obtain the conclusion that high pyrolysis is not conducive to generating furfural

(Cardoso and Ataide, 2015). The reason is that hemicellulose has the property of thermal instability compared to cellulose and lignin. Hemicellulose is almost completely decomposed at low pyrolysis temperature. While, cellulose and lignin only slightly decompose. The lots of furfural is generated at low pyrolysis temperature. Therefore, furfural is the major pyrolysis product in bio-oil at low pyrolysis temperature. Lu et al. pointed out that poplar wood impregnated with ZnCl_2 produces large content of furfural at low temperature, which is consistent with our work (Lu et al., 2011). It can be explained that ZnCl_2 can alter the competitiveness of possible furfural formation pathways and reduce the activation energy of the furfural generation pathways to generate furfural based on computational and experimental results (Hu et al., 2021). Furfural is one of the value-added compounds produced in catalytic biomass pyrolysis process (Bai et al., 2019). Therefore, bio-oil has commercial valuable due to fact that it has large content of the furfural (Lu et al., 2020). Besides, bio-oil has large content of ethylbenzene, p-xylene and m-xylene as pyrolysis temperature increases. Therefore, bio-oil has potential application in chemical intermediates (Lu et al., 2020).

3.4. Bio-gas analysis

The bio-gas component produced from different pyrolysis temperatures is shown in Fig. 3a. CH_4 content is increase at 400–600 °C and then decreases at 600–800 °C. Bio-gas has the maximum content of the CH_4 , which is 10.48 %. The content of the CO is decrease at 400–500 °C and then increase after 500–800. It can be explained that cellulose and hemicellulose are easily converted the decarboxylation into CO owe to poor thermal stability at low pyrolysis temperature (Cheng et al., 2020). The cellulose and hemicellulose is almost completely decomposed at 400–500 °C. The decarbonylation of lignin may generate CO during aromatic condensation at high pyrolysis temperature. Therefore, the content of CO in biogas increases at 500–800 °C. Bio-gas produced from 800 °C has the maximum content of CO, which is 47.09%. This analysis result indicates that pyrolysis temperature has great influenced the component of bio-gas.

The variation trend of bio-gas composition can be explained by the primary pyrolysis process and secondary pyrolysis of pyrolysis products. The generation process of bio-gas includes two stages (Li et al., 2007; Dai et al., 2000).

Table 1 Composition and relative content of bio-oil in the existence of additive at 400–800 °C.

Item	Composition	400 °C	500 °C	600 °C	700 °C	800 °C
		Relative content (%)				
1	Furfural	17.08	15.92	10.47	10.51	8.23
2	Toluene	0.84	1.38	2.72	–	–
4	Ethylbenzene	–	14.42	18.21	9.59	13.92
5	Paraxylene	–	28.89	23.09	17.96	30.41
6	M-xylene	0.27	14.87	43.60	9.21	10.23
7	Methyl 2-furoate	2.06	3.20	1.75	2.08	3.61
8	Methyl benzoate	–	–	–	0.79	0.45
9	2,6-diisopropyl	0.76	2.32	–	–	–
10	Methyl hexadecanoate	1.05	2.71	–	–	–
11	Methyl benzoate	0.71	–	–	–	–
12	Pterin-6-carboxylic acid	0.22	0.46	0.37	0.29	0.16

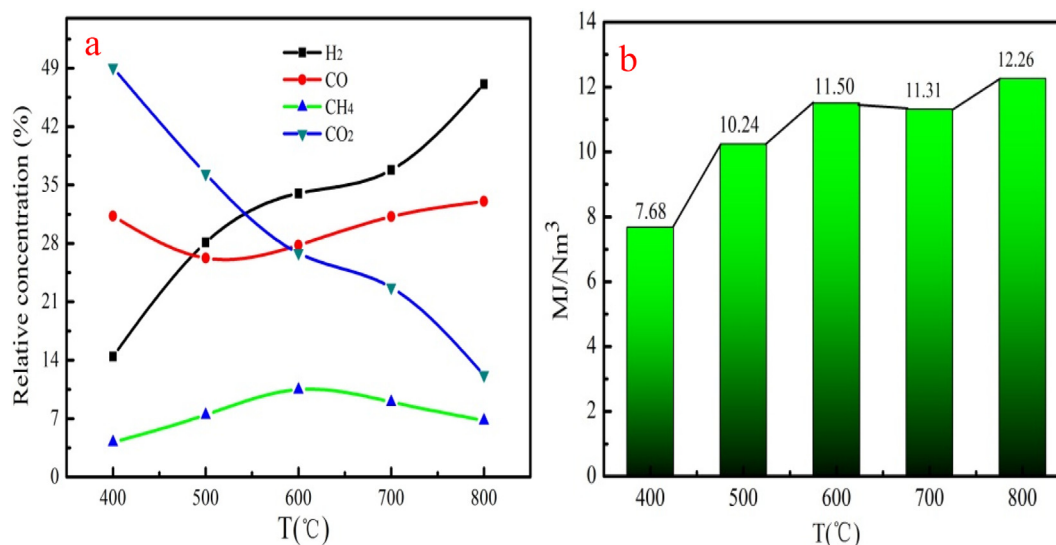
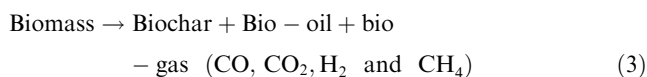


Fig. 3 The component (a) and heating value (b) of bio-gas at different pyrolysis temperatures.

Stage I: Primary pyrolysis of biomass. This stage occurs at low pyrolysis temperature. This stage can be explained by the following equation (Kellogg, 2002).



Stage II: The secondary pyrolysis and transformation of the bio-oil and bio-gas. This stage occurs at high pyrolysis temperature. The main chemical reactions of secondary pyrolysis and conversion of bio-oil include decarboxylation, decarboxylation, dehydrogenation, cyclization, aromatization and polymerization (Hong et al., 2017). Besides, these chemical reactions are generally promoted as pyrolysis temperature increases. Besides, bio-gas will undergo the secondary cracking and transformation, which produce lots of non-condensable gaseous at high pyrolysis temperature (Zhang et al., 2018; Foong et al., 2020).

Biochar reacts with CO₂ to generate CO, which is the reason that the yield of biochar decreases and CO content increases at high pyrolysis temperature. CH₄ also reacts with CO₂ to generate CO at high pyrolysis temperature, which leads to the content of the CH₄ decrease. The component of the bio-gas of WS/Fe/Zn without adding Fe(NO₃)₃ and ZnCl₂ under different pyrolysis temperature is shown in Fig. S2. Compared with WS/Fe/Zn pyrolysis without adding Fe(NO₃)₃ and ZnCl₂, Fe(NO₃)₃ contribute to the generation of H₂ in bio-gas. H₂ can be obtained from rearrangement reactions forming a polycyclic aromatic structure during the charring process but also by secondary reactions such as tar cracking and water gas shift reaction. Besides, the presence of Fe(NO₃)₃ the cracking of some depolymerization products could occur, which contributes to the production of the H₂. Collard et al. reported that bio-gas produced from cellulose mixed with Fe(NO₃)₃ has large content of H₂, which is consistent with our work (François-Xavier et al., 2015). The heating value of the bio-gas generally increases as pyrolysis temperature increases (Fig. 3b). As Fig. 3b shown, the maximum heating value of the bio-gas is 12.26 MJ/Nm.

3.5. Biochar analysis

The range of the Brunauer-Emmett-Teller (BET) surface area of biochars produced from 400 °C to 800 °C is 921.9–1556.7 m²/g. This result indicates that BET surface area of bio-char is increase before 700 °C, indicating that high pyrolysis temperature is conducive to generating a large number of pores (Zhang et al., 2018). However, BET surface area of biochar is decrease at 800 °C due to fact that the formed pore is ruined at 800 °C (Zhong et al., 2020). The pore volume of biochar at 400–800 °C is shown in Fig. 4. As Fig. 4 shown, the pore volume of the biochar also increases at 400–700 °C and then decreases after 700 °C. The biochar produced from 700 °C has the largest pore volume, which is 0.98 mL/g. This analysis result is consistent with BET surface area analysis.

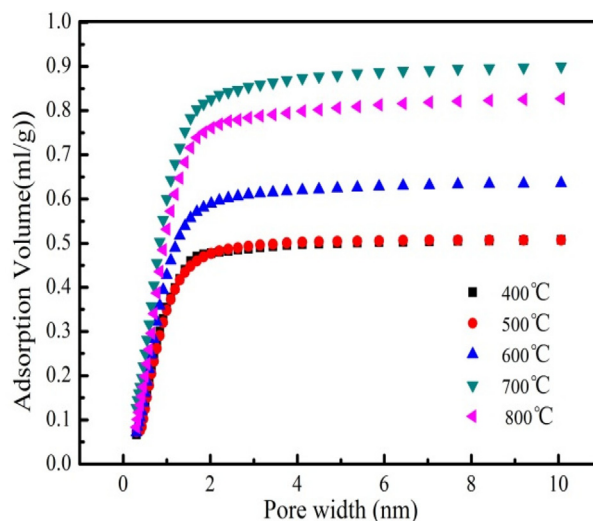


Fig. 4 Pore volume of the biochar at different pyrolysis temperatures.

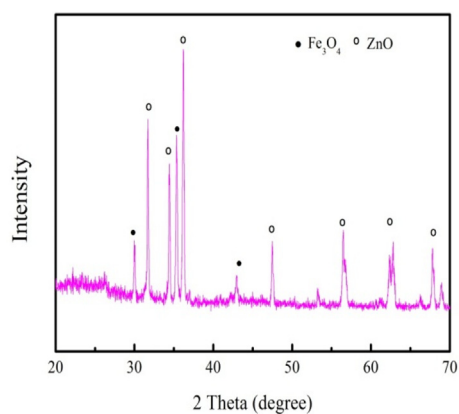


Fig. 5 XRD spectra of biochar produced from 700 °C.

The above analysis results indicate that the pore volume and surface area of biochar are significantly influenced by pyrolysis temperature. Biochar can be used in wastewater treatment owe to well-developed pore structure. The biochar produced form 700 °C is used as the candidate for further analysis and characterization owe to large surface area and pore volume.

The XRD spectra of biochar produced from 700 °C is shown in Fig. 5. As Fig. 5 shown, the biochar has ZnO and Fe₃O₄ characteristic peaks. The characteristic peaks of the ZnO and Fe₃O₄ are similar with the reported by the Qin et al. (Qin et al., 2017) when they prepared Fe₃O₄@SiO₂@-ZnO for photocatalytic 4-nitrophenol (Qin et al., 2017).

XRD analysis indicates that Fe(NO₃)₃ and ZnCl₂ are converted into the Fe₃O₄ and ZnO in the pyrolysis process, respectively. The high intensity of the ZnO peaks indicates that ZnO has well crystalline. Therefore, biochar could be employed as the photocatalyst for dyes removal due to the existence of ZnO. Fe₃O₄ peaks can be indexed to the diffraction pattern of (220), (311) and (400) planes. The biochar can be quickly recycled from aqueous solution after use under extra magnetic field owe to the existence of Fe₃O₄.

Fig. 6 shows the SEM and EDS images of biochar. Fig. 6a shows that biochar has developed pore structure. The surface of the biochar is existence of a great number of pores, which indicates that ZnCl₂ contributes to the formation of the pore during pyrolysis process. Yun et al. (Yun et al., 2022) pointed out that ZnCl₂ is the activation agent, which can promote to the formation of pore structure during activated carbon preparation process (Yun et al., 2022). As Fig. 6b shown, the surface of biochar has granular substance. The EDS images indicate that the granular substance has Fe, Zn and O elements. However, it does not have the Cl and N elements, indicating that the Fe(NO₃)₃ and ZnCl₂ occur decomposition reaction to remove the Cl and N elements. Fe(NO₃)₃ and ZnCl₂ form Fe₃O₄ and ZnO after decomposition reaction. This analysis result is consistent with XRD analysis.

3.6. The application of biochar in wastewater treatment

The biochar has ZnO/Fe₃O₄ and large BET surface area, which is employed as the adsorbent and photocatalyst for

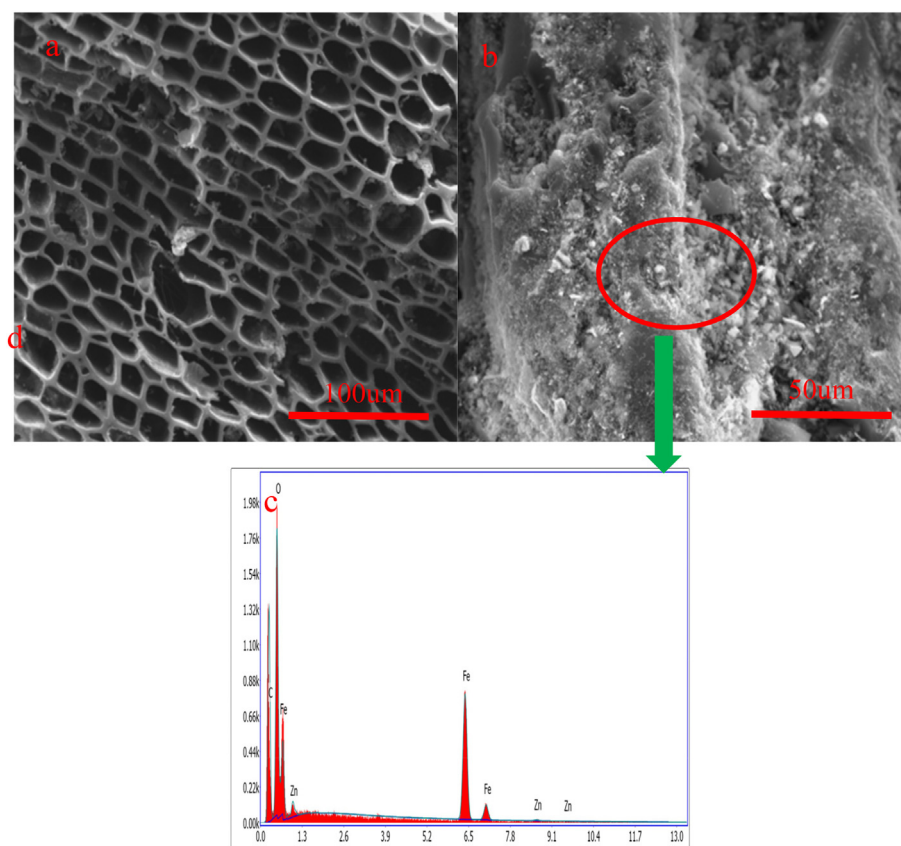
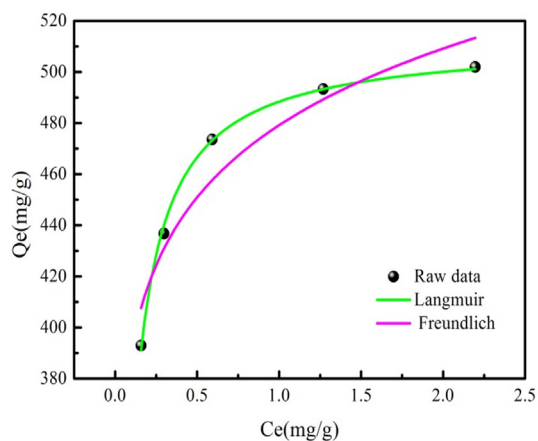


Fig. 6 SEM (a) and EDS (b) images of biochar.

Table 2 The adsorption isotherm parameters of the MO adsorption on biochar.

Isotherms	Parameters	Calculation results
Langmuir	Q_0 (mg/g)	512.29
	K_L (L/mg)	20.44
	R^2	0.9978
Freundlich	$1/n$	0.0876
	K_F ((mg/g).(L/mg) $^{1/n}$)	478.16
	R^2	0.8928

**Fig. 7** MO adsorption data fitting the Langmuir model.

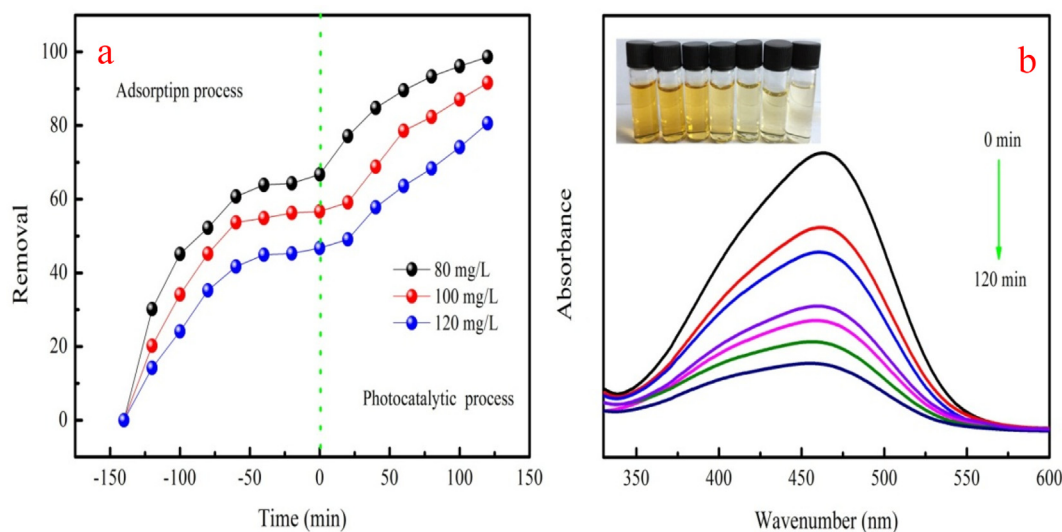
organic dye removal from wastewater. MO is used to investigate the adsorption/photocatalytic degradation performance of biochar. MO adsorption behavior on biochar is investigated by two kinds of adsorption isotherms (Abd El-Monaem et al., 2022). The parameters of adsorption isotherms are shown in Table S1. The corresponded calculation results are shown in Table 2; which is obtained from MO adsorption data fitting

adsorption isotherm models. As Table 2 shown, Langmuir isotherm model can be used to describe MO adsorption behavior on biochar with larger R^2 value (Omer et al., 2022). This result indicates that MO adsorption performance on biochar can be exactly predicted by the Langmuir isotherm model (Omer et al., 2022). MO adsorption capacity of biochar is 512.29 mg/g calculated from Langmuir isotherm model. Fig. 7 presents MO adsorption data fitting Langmuir model.

The photocatalytic degradation performance of the biochar is also investigated. Photodegradation experiments are conducted out in the dark condition before UV irradiation, which is used to eliminate the adsorption capacity of the biochar due to its large BET surface area. The adsorption and photodegradation process of biochar are shown in Fig. 8a. As Fig. 8a shown, biochar has certain of MO removal due to large BET surface area without UV irradiation at different concentrations. MO removal ranges from 46.73% to 66.70%, which is consistent with the adsorption experiment. MO photodegradation removals are increase as irradiation time increases at 80–120 mg/L. The removals of MO are 80.51–98.60% at 80–120 mg/L under UV light irradiation. The analysis results show that biochar has good MO photodegradation removal. The main peak intensity of MO also gradually decreases as irradiation time increases (Fig. 8b). This phenomenon indicates that MO structure is destroyed. Therefore, biochar is the promising photocatalyst for dye removal based on above analysis.

4. Conclusion

The influence of pyrolysis temperature on the physicochemical property of the pyrolysis products such as biochar, bio-oil and bio-gas is investigated at the 400–800 °C. High pyrolysis temperature promotes to produce bio-gas with the maximum yield of the 69.05% at 800 °C. The pyrolysis temperature significantly influences the composition and heating value of the bio-gas. Besides, the maximum heating value of the bio-gas is 12.26 MJ/Nm. However, bio-oil yield is little influenced by pyrolysis temperature. GC–MS analysis indicates that bio-oil mainly has furfural, ethylbenzene, p-xylene and m-xylene,

**Fig. 8** Adsorption and photodegradation process of the biochar (a) and UV-visible absorption spectra of biochar at the irradiation time (b).

which has potential application in chemical industries. The existence of ZnCl_2 contributes to the generation of the furfural. While, the presence of the of $\text{Fe}(\text{NO}_3)_3$ contributes to the generation of the H_2 . The BET surface area of biochar is influenced by pyrolysis temperature. The $\text{Fe}(\text{NO}_3)_3$ and ZnCl_2 are composed into Fe_3O_4 and ZnO in the pyrolysis process. Therefore, biochar can be used as the adsorbent and photocatalyst for MO removal from wastewater.

Declaration of Competing Interest

The authors declare that they have no known competing financial interests or personal relationships that could have appeared to influence the work reported in this paper.

Acknowledgments

The authors would like to express their gratitude to the Specialized Research Fund for the National Natural Science Foundation of China (51974110, 52074109, 52274261 and 21966019), Natural Science Foundation of Henan Province (232300420298), Key Scientific and Technological Project of Henan Province (222102320405), the Fundamental Research Funds for the Universities of Henan Province (NSFRF220417) for financial support, and we would like to thank the researchers in the Shiyanjia Lab (www.shiyanjia.com) for their helping with XRD analysis.

Appendix A. Supplementary material

Supplementary material to this article can be found online at <https://doi.org/10.1016/j.arabj.2023.104961>.

References

- Abd El-Monaem, E.M., Omer, A.M., El-Subruiti, G.M., Mohy-Eldin, M.S., Eltaweil, A.S., 2022. Zero-valent iron supported-lemon derived biochar for ultra-fast adsorption of methylene blue. *Biomass Convers. Biorefin.* 1, 2–9.
- Abdelsayed, V., Shekhawat, D., Smith, M.W., Link, D., Stiegman, A. E., 2018. Microwave-assisted pyrolysis of Mississippi coal: A comparative study with conventional pyrolysis. *Fuel* 217, 656–667.
- Ahmadpour, A., Do, D.D., 1997. The preparation of activated carbon from macadamia nutshell by chemical activation. *Carbon* 35 (12), 1723–1732.
- Bai, X., Li, J., Jia, C., Shao, J., Yang, Q., Chen, Y., Yang, H., Wang, X., Chen, H., 2019. Preparation of furfural by catalytic pyrolysis of cellulose based on nano Na/Fe-solid acid. *Fuel* 258, 116089.
- Branca, C., Blasi, C.D., Galgano, A., 2010. Pyrolysis of Corncobs Catalyzed by Zinc Chloride for Furfural Production. *Ind. Eng. Chem. Res* 49, 9743–9752.
- Cao, Y., Chen, S.S., Tsang, D.C., Clark, J.H., Zhang, S., 2020. Microwave-assisted depolymerization of various types of waste lignin over two-dimensional CuO/BCN catalysts. *Green Chem.* 22, 725–736.
- Cardoso, C.R., Ataide, C.H., 2015. Micropyrolysis of Tobacco Powder at 500 degrees C: Influence of ZnCl_2 and MgCl_2 Contents on the Generation of Products. *Chem. Eng. Commun.* 202, 484–492.
- Chen, P., Xie, Q., Addy, M., Zhou, W., Liu, Y., Wang, Y., Cheng, Y., Li, K., Ruan, R., 2016. Utilization of municipal solid and liquid wastes for bioenergy and bioproducts production. *Bioresour. Technol.* 215, 163–172.
- Cheng, S., Zhang, L., Zhang, L., Xia, H., Xia, H., Peng, J., Peng, J., Shu, J., Shu, J., 2017. Adsorption behavior of methylene blue onto waste-derived adsorbent and exhaust gases recycling. *RSC Adv.* 7, 27331–27341.
- Cheng, S., Zhang, Q., Shu, J.H., Xia, H.Y., Zhang, L.B., Peng, J.H., Lin, G., Hu, W.H., Chen, Q., 2020. Microwave-assisted catalytic pyrolysis of the Eupatorium adenophorum for obtaining valuable products. *Environ. Prog. Sustain. Energy* 39, 2–12.
- Cheng, S., Liu, Y., Xing, B., Qin, X., Zhang, C., Xia, H., 2021. Lead and cadmium removal from wastewater by sustainable biochar derived from poplar saw dust. *J. Clean. Prod.* 314, 128074.
- Cheng, S., Zhao, S., Xing, B., Shi, C., Meng, W., Zhang, C., Bo, Z., 2022. Facile one-pot green synthesis of magnetic separation photocatalyst-adsorbent and its application. *J. Water Process Eng.* 47, 102802.
- Cheng, S., Zhao, S., Xing, B., Liu, Y., Zhang, C., Xia, H., 2022. Preparation of magnetic adsorbent-photocatalyst composites for dye removal by synergistic effect of adsorption and photocatalysis. *J. Clean. Prod.* 348, 131301.
- Cheng, S., Meng, M., Xing, B., Shi, C., Nie, Y., Xia, D., Yi, G., Zhang, C., Xia, H., 2022. Preparation of valuable pyrolysis products from poplar waste under different temperatures by pyrolysis: Evaluation of pyrolysis products. *Bioresour. Technol.* 364, 128011.
- Cherubini, F., Ulgiati, S., 2010. Crop residues as raw materials for biorefinery systems – A LCA case study. *Appl. Energy* 87, 47–57.
- Dai, X., Wu, C., Li, H., Chen, Y., 2000. The Fast Pyrolysis of Biomass in CFB Reactor. *Energy Fuels* 14, 552–557.
- Durak, H., Genel, S., 2020. Catalytic hydrothermal liquefaction of lactuca scariola with a heterogeneous catalyst: The investigation of temperature, reaction time and synergistic effect of catalysts. *Bioresour. Technol.* 309, 123375.
- Foong, S.Y., Liew, R.K., Yang, Y., Cheng, Y.W., Su, S.L., 2020. Valorization of biomass waste to engineered activated biochar by microwave pyrolysis: Progress, challenges, and future directions. *Chem. Eng. J.* 389, 124401.
- Foong, S.Y., Liew, R.K., Yang, Y., Cheng, Y.W., Yek, P.N.Y., Mahari, W.A.W., Lee, X.Y., Han, C.S., Vo, D.-V.-N., Quyet Van, L., Aghbashlo, M., Tabatabaei, M., Sonne, C., Peng, W., Lam, S. S., 2020. Valorization of biomass waste to engineered activated biochar by microwave pyrolysis: Progress, challenges, and future directions. *Chem. Eng. J.* 389, 124401.
- François-Xavier, C., Ammar, B., Martin, D., Ghislaine, V., Joël, B., 2015. Influence of impregnated iron and nickel on the pyrolysis of cellulose. *Biomass Bioenergy* 80, 52–62.
- Gautam, R., Shyam, S., Reddy, B.R., Govindaraju, K., Vinu, R., 2019. Microwave-assisted pyrolysis and analytical fast pyrolysis of macroalgae: product analysis and effect of heating mechanism. *Sustainable Energy Fuels* 3, 3009–3020.
- Ge, S., Foong, S.Y., Ma, N.L., Liew, R.K., Mahari, W.A.W., Xia, C., Yek, P.N.Y., Peng, W., Nam, W.L., Lim, X.Y., Liew, C.M., Chong, C.C., Sonne, C., Lam, S.S., 2020. Vacuum pyrolysis incorporating microwave heating and base mixture modification: An integrated approach to transform biowaste into eco-friendly bioenergy products. *Renew. Sustain. Energy Rev.* 127, 109871.
- Hong, Y., Chen, W., Luo, X., Pang, C., Lester, E., Wu, T., 2017. Microwave-enhanced pyrolysis of macroalgae and microalgae for syngas production. *Bioresour. Technol.* 237, 47–56.
- Hou, L., Xing, B., Zeng, H., Kang, W., Guo, H., Cheng, S., Huang, G., Cao, Y., Chen, Z., Zhang, C., 2022. Aluminothermic reduction synthesis of Si/C composite nanosheets from waste vermiculite as high-performance anode materials for lithium-ion batteries. *J. Alloys Compd.*, 166134.
- Hou, J., Zhong, D., Liu, W., 2022. Catalytic co-pyrolysis of oil sludge and biomass over ZSM-5 for production of aromatic platform chemicals. *Chemosphere* 291.
- Hu, B., Xie, W.L., Wu, Y.T., Liu, J., Ma, S.W., Wang, T.P., Zheng, S., Lu, Q., 2021. Mechanism study on the formation of furfural during zinc chloride-catalyzed pyrolysis of xylose. *Fuel* 295, 120656.

- Kan, T., Strezov, V., Evans, T., He, J., Kumar, R., Lu, Q., 2020. Catalytic pyrolysis of lignocellulosic biomass: A review of variations in process factors and system structure. *Renew. Sustain. Energy Rev.* 134, 110305.
- Kellogg, W.D., 2002. Pyrolysis behavior and kinetics of biomass derived materials. *J. Anal. Appl. Pyrolysis* 62, 331–349.
- Li, H., Li, J., Fan, X., Li, X., Gao, X., 2019. Insights into the synergetic effect for co-pyrolysis of oil sands and biomass using microwave irradiation. *Fuel* 239, 219–229.
- Li, Y., Nishu, Y.D., Li, C., Liu, R., 2022. Deactivation mechanism and regeneration effect of bi-metallic Fe-Ni/ ZSM-5 catalyst during biomass catalytic pyrolysis. *Fuel* 312 (122924).
- Li, J., Yan, R., Xiao, B., Wang, X., Yang, H., 2007. Influence of temperature on the formation of oil from pyrolyzing palm oil wastes in a fixed bed reactor. *Energy Fuel* 21, 2398–2407.
- Lu, Q., Dong, C.Q., Zhang, X.M., Tian, H.Y., Yang, Y.P., Zhu, X.F., 2011. Selective fast pyrolysis of biomass impregnated with ZnCl₂ to produce furfural: Analytical Py-GC/MS study. *J. Anal. Appl. Pyrolysis* 90, 204–212.
- Lu, Q., Dong, C.-Q., Zhang, X.-M., Tian, H.-Y., Yang, Y.-P., Zhu, X.-F., 2011. Selective fast pyrolysis of biomass impregnated with ZnCl₂ to produce furfural: Analytical Py-GC/MS study. *J. Anal. Appl. Pyrolysis* 90, 204–212.
- Lu, Q., Yuan, S., Liu, C., Zhang, T., Xie, X., Deng, X., He, R., 2020. A Fe-Ca/SiO₂ catalyst for efficient production of light aromatics from catalytic pyrolysis of biomass. *Fuel* 279, 118500.
- Nma, B., Hms, A., Shta, C., Nam, D., Akga, E., Chi, H., Mrs, A., Yun, T., 2022. Catalytically active metal oxides studies for the conversion technology of carboxylic acids and bioresource based fatty acids to ketones: A review. *Bioresour. Technol. Rep.* 100988
- Oh, S.J., Jung, S.H., Kim, J.S., 2013. Co-production of furfural and acetic acid from corn cob using ZnCl₂ through fast pyrolysis in a fluidized bed reactor. *Bioresour. Technol.* 144, 172–178.
- Omer, A.M., Dey, R., Eltaweil, A.S., Abd El-Monaem, E.M., Ziora, Z.M., 2022. Insights into recent advances of chitosan-based adsorbents for sustainable removal of heavy metals and anions. *Arab. J. Chem.* 15, 103543.
- Omer, A.M., El-Monaem, E.M.A., Eltaweil, A.S., 2022. Novel reusable amine-functionalized cellulose acetate beads impregnated aminated graphene oxide for adsorptive removal of hexavalent chromium ions. *Int. J. Biol. Macromol.* 208, 925–934.
- Ouyang, S., Xiong, D., Xie, Y., Ma, L., Hao, Z., Sun, B., Yang, J., Chen, W., Li, X., 2019. Thermogravimetric kinetic analysis and demineralization of chars from pyrolysis of scrap tire pretreated by waste coal tar. *Energy Sources Part A-Recovery Utiliz. Environ. Effects*, 1–17.
- Pang, Z.B., Wang, J.G., Cui, H.Y., Wang, J.H., 2023. In situ catalytic pyrolysis of pine powder by ZnCl₂ to bio-oil under mild conditions and application of biochar. *J. Fuel Chem. Technol.*, 1–9
- Prashanth, P.F., Kumar, M.M., Vinu, R., 2020. Analytical and Microwave Pyrolysis of Empty Oil Palm Fruit Bunch: Kinetics and Product Characterization. *Bioresour. Technol.* 310, 123394.
- Qin, Y., Zhang, H., Tong, Z., Song, Z., Chen, N., 2017. A facile synthesis of Fe₃O₄@SiO₂@ZnO with superior photocatalytic performance of 4-nitrophenol. *J. Environ. Chem. Eng.* 5, 2207–2213.
- Reddy, B.R., Shravani, B., Das, B., Dash, P.S., Vinu, R., 2019. Microwave-assisted and analytical pyrolysis of coking and non-coking coals: Comparison of tar and char compositions. *J. Anal. Appl. Pyrolysis* 142, 104611–104619.
- Ren, X., Ghazani, M.S., Zhu, H., Ao, W., Zhang, H., Moreside, E., Zhu, J., Yang, P., Zhong, N., Bi, X., 2022. Challenges and opportunities in microwave-assisted catalytic pyrolysis of biomass: A review. *Appl. Energy* 315, 118970.
- Robinson, J., Dodds, C., Stavrinides, A., Kingman, S., Katrib, J., Wu, Z., Medrano, J., Overend, R., 2015. Microwave Pyrolysis of Biomass: Control of Process Parameters for High Pyrolysis Oil Yields and Enhanced Oil Quality. *Energy Fuel* 29, 1701–1709.
- Rolin, A., Tichard, C., Masson, D., Deglise, X., 1983. Catalytic conversion of biomass by fast pyrolysis. *J. Anal. Appl. Pyrolysis* 5, 151–166.
- Ryu, H.W., Kim, D.H., Jae, J., Lam, S.S., Park, E.D., Park, Y.-K., 2020. Recent advances in catalytic co-pyrolysis of biomass and plastic waste for the production of petroleum-like hydrocarbons. *Bioresour. Technol.* 310, 123473.
- Shi, K., Wu, T., Zhao, H., Lester, E., Hall, P., 2013. Microwave Induced Pyrolysis of Biomass. *Appl. Mech. Mater.* 319, 127–133.
- Song, Q.H., Nie, J.Q., Ren, M.G., Guo, Q.X., 2000. Effective Phase Separation of Biomass Pyrolysis Oils by Adding Aqueous Salt Solutions. *Energy Fuel* 23, 3307–3312.
- Stefanidis, S.D., Kalogiannis, K.G., Iliopoulou, E.F., Lappas, A.A., Pilavachi, P.A., 2011. In-situ upgrading of biomass pyrolysis vapors: Catalyst screening on a fixed bed reactor. *Bioresour. Technol.* 102, 8261–8267.
- Sun, K., Huang, Q., Chi, Y., Yan, J., 2018. Effect of ZnCl₂-activated biochar on catalytic pyrolysis of mixed waste plastics for producing aromatic-enriched oil. *Waste Manag.* 81, 128–137.
- Tang, Y.H., Liu, S.H., Tsang, D.C.W., 2020. Microwave-assisted production of CO₂-activated biochar from sugarcane bagasse for electrochemical desalination. *J. Hazard. Mater.* 383, 121192.
- Wang, Y., Dai, L., Wang, R., Fan, L., Liu, Y., Xie, Q., Ruan, R., 2016. Hydrocarbon fuel production from soapstock through fast microwave-assisted pyrolysis using microwave absorbent. *J. Anal. Appl. Pyrolysis* 119, 251–258.
- Xia, H.Y., Lei, S., Lu, W., Cai, N., Xiao, H., Chen, Y., Chen, H., 2023. Iron salt catalytic pyrolysis of biomass: Influence of iron salt type. *Energy* 262, 125415.
- Xie, Q.L., Peng, P., Liu, S.Y., Min, M., Cheng, Y.L., Wan, Y.Q., Li, Y., Lin, X.Y., Liu, Y.H., Chen, P., 2014. Fast microwave-assisted catalytic pyrolysis of sewage sludge for bio-oil production. *Bioresour. Technol.* 172, 162–168.
- Yang, Y., Liew, R.K., Tamothran, A.M., Foong, S.Y., Yek, P.N.Y., Chia, P.W., Tran, T.V., Peng, W., Lam, S.S., 2021. Gasification of refuse-derived fuel from municipal solid waste for energy production: a review. *Environ. Chem. Lett.* 19, 2127–2140.
- Yun, H., Kim, Y.J., Bin Kim, S., Yoon, H.J., Kwak, S.K., Lee, K.B., 2022. Preparation of copper-loaded porous carbons through hydrothermal carbonization and ZnCl₂ activation and their application to selective CO adsorption: Experimental and DFT calculation studies. *J. Hazard. Mater.* 426, 127816.
- Zeng, H., Xing, B., Cao, Y., Xu, B., Hou, L., Guo, H., Cheng, S., Huang, G., Zhang, C., Sun, Q., 2022. Insight into the microstructural evolution of anthracite during carbonization-graphitization process from the perspective of materialization. *Int. J. Min. Sci. Technol.* 12, 3–13.
- Zhang, X., Che, Q.F., Cui, X., Wei, Z.Y., Zhang, X.Y., Chen, Y. Q., Wang, X.H., Chen, H.P., 2018. Application of biomass pyrolytic polygeneration by a moving bed: Characteristics of products and energy efficiency analysis. *Bioresour. Technol.* 254, 130–138.
- Zhang, X., Che, Q., Cui, X., Wei, Z., Zhang, X., Chen, Y., Wang, X., Chen, H., 2018. Application of biomass pyrolytic polygeneration by a moving bed: Characteristics of products and energy efficiency analysis. *Bioresour. Technol.* 254, 130–138.
- Zhang, C., Li, S., Ouyang, S., Tsang, C.-W., Xiong, D., Yang, K., Zhou, Y., Xiao, Y., 2021. Co-pyrolysis characteristics of camellia oleifera shell and coal in a TGA and a fixed-bed reactor. *J. Anal. Appl. Pyrolysis* 155, 105035.
- Zhong, Z., Lu, X., Yan, R., Lin, S., Wu, X., Huang, M., Liu, Z., Zhang, F., Zhang, B., Zhu, H., 2020. Phosphate sequestration by magnetic La-impregnated bentonite granules: A combined experimental and DFT study. *Sci. Total Environ.* 738, 139636.